



Assessing the performance of AI-assisted technicians in liver segmentation, Couinaud division, and lesion detection: a pilot study

Luis Núñez¹ · Carlos Ferreira¹ · Amirkasra Mojtahed² · Hildo Lamb³ · Stefano Cappio⁵ · Mohammad Ali Husainy⁴ · Andrea Dennis¹ · Michele Pansini^{4,5}

Received: 15 April 2024 / Revised: 16 July 2024 / Accepted: 21 July 2024 / Published online: 10 August 2024
© The Author(s) 2024

Abstract

Background In patients with primary and secondary liver cancer, the number and sizes of lesions, their locations within the Couinaud segments, and the volume and health status of the future liver remnant are key for informing treatment planning. Currently this is performed manually, generally by trained radiologists, who are seeing an inexorable growth in their workload. Integrating artificial intelligence (AI) and non-radiologist personnel into the workflow potentially addresses the increasing workload without sacrificing accuracy. This study evaluated the accuracy of non-radiologist technicians in liver cancer imaging compared with radiologists, both assisted by AI.

Methods Non-contrast T1-weighted MRI data from 18 colorectal liver metastasis patients were analyzed using an AI-enabled decision support tool that enables non-radiology trained technicians to perform key liver measurements. Three non-radiologist, experienced operators and three radiologists performed whole liver segmentation, Couinaud segment segmentation, and the detection and measurements of lesions aided by AI-generated delineations. Agreement between radiologists and non-radiologists was assessed using the intraclass correlation coefficient (ICC). Two additional radiologists adjudicated any lesion detection discrepancies.

Results Whole liver volume showed high levels of agreement between the non-radiologist and radiologist groups (ICC = 0.99). The Couinaud segment volumetry ICC range was 0.77–0.96. Both groups identified the same 41 lesions. As well, the non-radiologist group identified seven more structures which were also confirmed as lesions by the adjudicators. Lesion diameter categorization agreement was 90%, Couinaud localization 91.9%. Within-group variability was comparable for lesion measurements.

Conclusion With AI assistance, non-radiologist experienced operators showed good agreement with radiologists for quantifying whole liver volume, Couinaud segment volume, and the detection and measurement of lesions in patients with known liver cancer. This AI-assisted non-radiologist approach has potential to reduce the stress on radiologists without compromising accuracy.

✉ Luis Núñez
luis.nunez@perspectum.com

¹ Perspectum Ltd., Gemini One, 5520 John Smith Drive, Oxford OX4 2LL, UK

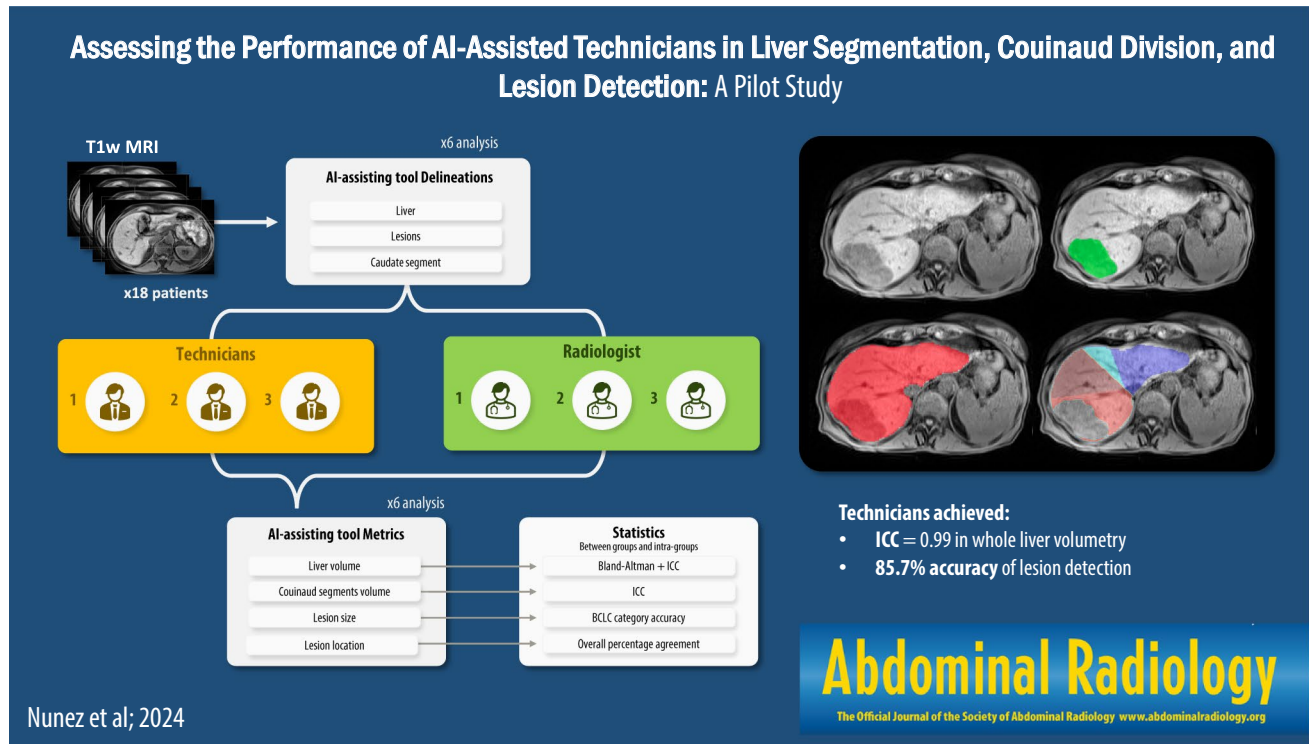
² Division of Abdominal Imaging, Harvard Medical School, Massachusetts General Hospital, Boston, MA, USA

³ Department of Radiology, Leiden University Medical Centre, Leiden, The Netherlands

⁴ Department of Radiology, Oxford University Hospitals NHS Foundation Trust, Oxford, UK

⁵ Clinica Di Radiologia EOC, Istituto Di Imaging Della Svizzera Italiana (IIMSI), Lugano, Switzerland

Graphical abstract



Keywords Liver cancer · MRI · Artificial Intelligence · Lesion detection · Colorectal liver metastases · Liver segmentation · Radiology efficiency

Introduction

Liver malignancy is ranked as the fifth and ninth most prevalent cancer among males and females respectively, and globally is the second leading cause of cancer-related mortality [1, 2]. Accurate and timely imaging analysis is crucial for therapeutic planning, whether for primary liver tumours such as hepatocellular carcinoma (HCC) or secondary lesions originating from other organs, particularly the colon, breast, or lung [3]. In the West, liver metastatic cancers are more frequent than primary tumours, although the incidence of HCC is rising rapidly; HCC is dominant in Asia [3]. Treatment selection for both primary and secondary liver cancers is based on established guidelines such as BCLC [4], AASLD [5], EASL [6], and APASL [7]. The main curative approach for primary HCC is surgical resection, whereas liver metastases are often treated with neoadjuvant chemotherapy or regional radiotherapy [8]. Detailed quantitative assessment of a lesion's characteristics and location, as well as assessment of the future liver remnant, are therefore required for determining an appropriate course of treatment.

However, such assessments take time, while radiologists are already struggling with ever-increasing workload [9, 10],

that has grown consistently over the past fifteen years [11]. This surge is driven in part by the rapidly growing utilization of diagnostic imaging modalities, particularly magnetic resonance imaging (MRI) and computed tomography (CT) [9, 11]. Burnout is now a pressing concern with a recent estimate of as many as 34% of radiologists reporting high levels of occupational stress and extended working hours [12, 13].

To address these challenges, new clinical practice strategies are being explored. Specifically, in the realm of hepatic oncology management, AI-assisted techniques employing deep learning algorithms have demonstrated capability to provide preliminary delineations of the liver, Couinaud segments, and identifiable lesions [14]. Such AI-generated contours can be edited and refined, improving inter-operator agreement, and reducing the time previously expended by radiologists on manual segmentation tasks.

In this study, we investigate an approach to alleviate radiological workload without compromising on quality. Non-radiologist but experienced technicians, assisted by an AI-enabled software tool that provides initial segmentation suggestions, were tasked with performing hepatic segmentation, Couinaud segment division for volumetry and lesion detection, and measurement. Their accuracy was compared

to that of experienced radiologists. The goal of the work is to evaluate the potential of this AI-assisted approach to enhance radiology workflow efficiency without compromising analytical quality.

Methods

Data acquisition

This study utilized non-contrast T1-weighted (T1w) MRI data from 18 patients with confirmed diagnoses of colorectal liver metastases. The scans were acquired as part of the Precision1 clinical trial (NCT04597710) using a Siemens 1.5 Tesla Aera scanner. The MRI scans were an integral component of the treatment planning process at the time of acquisition.

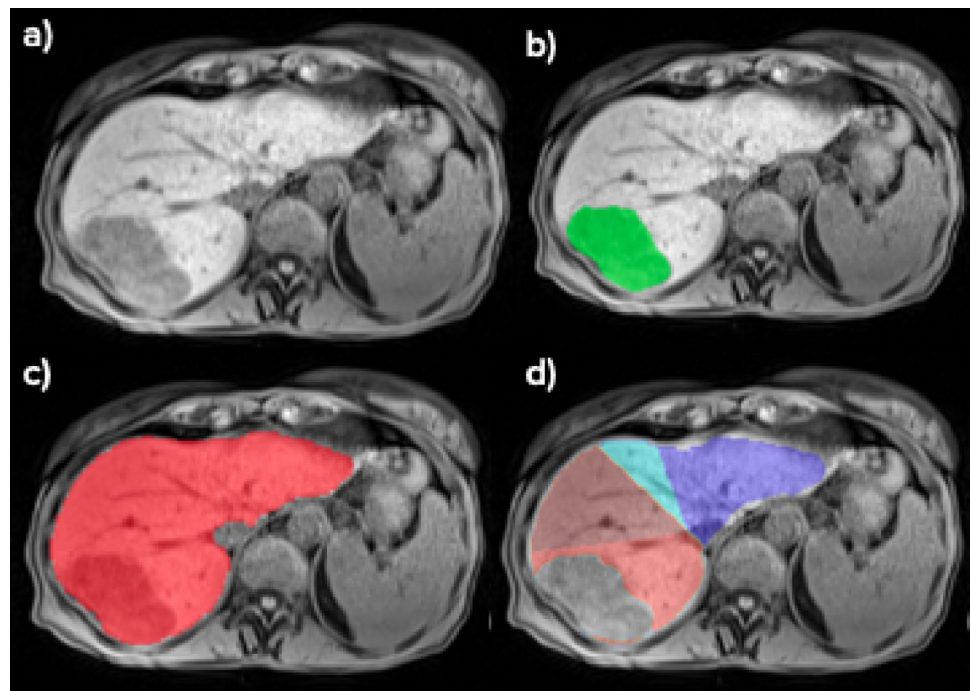
Image analysis protocol

T1 weighted scans were analyzed independently by a total of 6 individuals—3 experienced technicians (“analysts”) and 3 radiologists. All 6 readers utilized Hepatica™ software (Perspectum Ltd, Oxford, UK, trademarked in the UK and Europe region), an AI-enabled decision support tool designed for liver imaging analysis. The Hepatica software uses a convolutional neural network (CNN) to automatically delineate the liver, including the caudate lobe, from the 3D MRI data (Example in Fig. 1). The analysts fine-tuned these AI-generated segmentations using

the software's manual editing tools. For Couinaud segmentation, each analyst manually positioned eight predefined anatomical landmarks within the tool's interactive 3D visualization interface. These landmarks included the inferior vena cava (superior and inferior zones), middle hepatic vein, gallbladder fossa, right hepatic vein, umbilical fissure, and the right and left portal veins. The software then automatically calculates the planes dividing the liver into the nine Couinaud segments based on combinations of these user-provided landmarks and the caudate segmentation [15]. In addition to liver segmentation, the software provides initial delineations of any suspected lesions within the liver parenchyma. The AI-assisted tool used in this study was specifically trained on non-contrast T1w images, leveraging advanced deep learning techniques to enhance lesion detectability even without contrast [14].

The analysts refined these AI-generated lesion contours and manually removed incorrect detections (false positives) and delineated any additional lesions missed by the AI (false negatives). All analysts had knowledge of a confirmed cancer diagnosis but were otherwise blinded to the patients' clinical information. Each analyst conducted their analyses independently to ensure unbiased assessments. The technicians underwent twelve hours of anatomy training prior to commencing analysis, this included liver anatomy, vascular anatomy, Couinaud division, and fundamental principles of liver assessment by MRI. Both groups received three hours of specific training to ensure proficiency with the AI-assisted Quantitative Multiparametric MRI tool. The analysis workflow is depicted in Fig. 2.

Fig. 1 Example of segmentations generated by analysts. **a** Slice of patient with colorectal liver metastases. **b** Tumour segmented in green. **c** Liver segmented in red. **d** Couinaud segmentation of the liver, after removing the lesion from the delineation mask. Red represents segment 7, maroon represents segment 8, Light blue represents segment 4a and navy represents segment 2



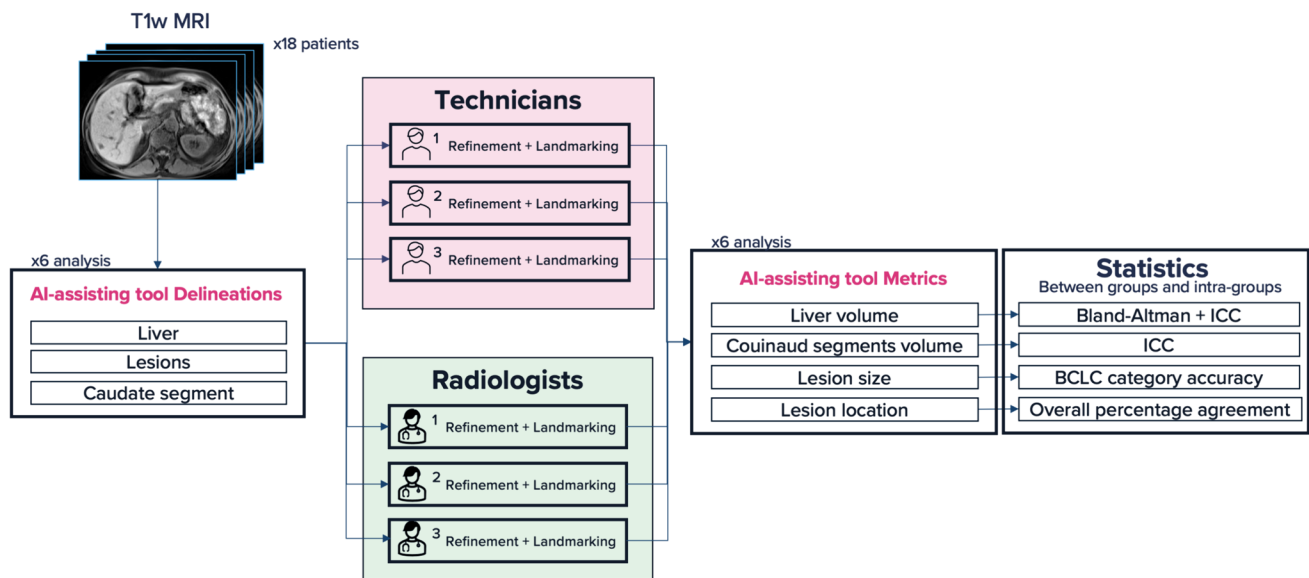


Fig. 2 Overview of the study workflow comparing the performance of AI-assisted technicians and radiologists in liver cancer imaging analysis. The AI-assisted tool (Hepatica, Perspectum Ltd, Oxford, UK) provides initial segmentations of the liver, Couinaud segments, and lesions, which are then refined by the raters. Raters also manu-

ally place anatomical landmarks for Couinaud segmentation. The tool extracts metrics from the raters' outputs, enabling statistical comparisons between and within the technician and radiologist groups to assess the accuracy and agreement of the AI-assisted approach

Statistical analysis

Interclass correlation coefficients (ICCs) were calculated to assess agreement between the non-radiologist and radiologist groups for whole liver volume and Couinaud segment volumetry. Bland–Altman plots were used to evaluate bias and limits of agreement (LOA) for whole liver volume measurements. Lesion detection accuracy was determined using the majority vote of the three radiologists as the ground truth. To measure agreement on lesion size measurement, a set of categories was defined according to thresholds present in the decision tree of the Barcelona Clinic Liver Cancer (BCLC) staging system [4]: < 2 cm, 2–3 cm, 3–4 cm, and 4–8 cm. Agreement on the category assigned by each group was measured as follows. The overall percentage agreement between the non-radiologist and radiologist groups in detecting the presence of lesions within each Couinaud segment was calculated. For lesions identified solely by the non-radiologist group, an adjudication panel consisting of two additional radiologists, reviewed the MRI scans and the delineated lesions in order to assess their validity. The diagnostic accuracy, sensitivity, and specificity of the non-radiologist group in detecting lesions were calculated using the adjudicated results as the reference standard. The inter-rater variability within each group was assessed for whole liver and Couinaud segment volume, lesion size categorization and Couinaud segment presence using pairwise comparisons of the three members of each group.

Results

A total of 18 patient data are included in the full analysis (median age of 66 years, 50% female). All patients had colorectal liver metastases. Mean liver volume was 1642 ± 443 ml with an average of 2.67 lesions per patient.

Agreement regarding lesion size categorization for each combination ranged between 0.80, 0.83, and 0.68 for radiologists and 0.72, 0.68, and 0.68 within the non-radiologist groups. Agreements in Couinaud locations of the lesions were 84.9%, 80.2%, and 82.4% for radiologists and 88%, 85.4%, and 83.3% for analysts.

There was good agreement in the measures of whole liver volume between the groups, with an ICC of 0.99, a low bias of -0.06%, and LOA of [-1.49%, 1.42%] (Fig. 3). For Couinaud segments, ICC ranged from 0.767 in segment 4b to 0.961 in segment 8. Each group's variability is detailed in Table 1.

A total of 41 lesions were identified by both radiologists and analysts. The non-radiologist analysts detected an additional 15 structures, 7 were considered lesions and 8 non-lesions by the adjudicator panel. Using the adjudicator assessment as ground truth, the analysts had an overall diagnostic accuracy of 85.7%, with 100% sensitivity and 85.7% specificity. When including the lesions not initially detected by the radiologists but later included after adjudication, they reached an accuracy of 87.5%, with 85.4% sensitivity and 100% specificity (Summarized in Fig. 4).

Fig. 3 Bland–Altman comparison of similarity in whole liver volume measurements between mean of technicians and radiologists. dotted light-blue line represents bias (− 0.06%) and dotted navy line represents upper and lower LOA (− 1.49%, 1.42%)

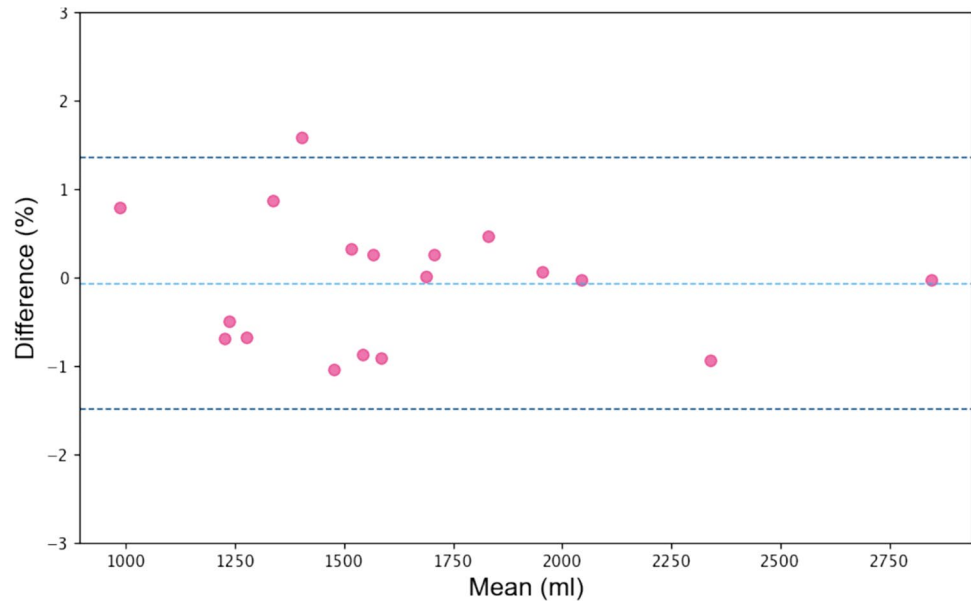


Table 1 Summary of agreement between radiologists and technician groups and agreement within each group

| Metric | Mean Rad vs Mean Tec | Tec1 vs Tec2 | Tec1 vs Tec3 | Tec3 vs Tec2 | Rad1 vs Rad2 | Rad1 vs Rad3 | Rad2 vs Rad3 |
|--|----------------------|--------------|--------------|--------------|--------------|--------------|--------------|
| Whole liver volume (ICC) | 0.999 | 0.999 | 0.999 | 0.999 | 0.999 | 0.999 | 0.998 |
| Sg1 liver volume (ICC) | 0.887 | 0.932 | 0.873 | 0.751 | 0.978 | 0.981 | 0.944 |
| Sg2 liver volume (ICC) | 0.935 | 0.871 | 0.904 | 0.848 | 0.911 | 0.872 | 0.872 |
| Sg3 liver volume (ICC) | 0.941 | 0.850 | 0.857 | 0.899 | 0.899 | 0.876 | 0.786 |
| Sg4a liver volume (ICC) | 0.885 | 0.859 | 0.871 | 0.955 | 0.820 | 0.856 | 0.901 |
| Sg4b liver volume (ICC) | 0.767 | 0.877 | 0.848 | 0.784 | 0.595 | 0.643 | 0.766 |
| Sg5 liver volume (ICC) | 0.932 | 0.863 | 0.876 | 0.907 | 0.859 | 0.829 | 0.695 |
| Sg6 liver volume (ICC) | 0.873 | 0.895 | 0.948 | 0.849 | 0.857 | 0.752 | 0.71 |
| Sg7 liver volume (ICC) | 0.951 | 0.929 | 0.887 | 0.896 | 0.878 | 0.757 | 0.766 |
| Sg8 liver volume (ICC) | 0.961 | 0.945 | 0.954 | 0.908 | 0.923 | 0.885 | 0.824 |
| Lesion diameter (category accuracy) | 0.9 | 0.68 | 0.80 | 0.83 | 0.68 | 0.68 | 0.72 |
| Lesion couinaud segment location (OPA) | 91.9 | 88 | 85.4 | 83.3 | 84.9 | 80.2 | 82.4 |

Both groups agreed on the presence of lesions in Couinaud segments in 91.9% of cases.

The 41 lesions detected by both groups ranged in volume between 1.3 ml and 43.4 ml and diameter of 1.1–5.1 cm. Out of the 41 lesions, 90% of the lesions were assigned the same size category when comparing the mean diameter of each group lesions there was agreement between lesion size grouping based on the mean diameter (Fig. 5).

Discussion

The primary aim of this study was to assess the accuracy of trained technicians in performing liver segmentation, Couinaud segmentation and lesion detection and delineation. The experienced technicians' performance was compared with that of experienced radiologists, with a

| | Radiologists | | | Technicians | | |
|------------|----------------------------|---------------|-----------------------------|-----------------------------|---------------|----------------------------|
| | Segmented | Not Segmented | | Segmented | Not Segmented | |
| Lesion | 41 | 7 | Sensitivity 41/48(85.4%) | 48 | 0 | Sensitivity 48/48(100%) |
| Not lesion | 0 | 8 | | 8 | 0 | |
| | Specificity 41/41(100%) | | Accuracy 49/56(87.5%) | Specificity 48/56(85.7%) | | Accuracy 48/56(85.7%) |

Fig. 4 Comparative performance metrics between radiologists and technicians in lesion segmentation. The table displays the number of lesions correctly segmented (true positives) and missed (false negatives), along with the number of non-lesion regions accurately left

unsegmented (true negatives) and incorrectly segmented (false positives). Sensitivity, specificity, and accuracy percentages are calculated based on these values to evaluate the diagnostic performance of each group

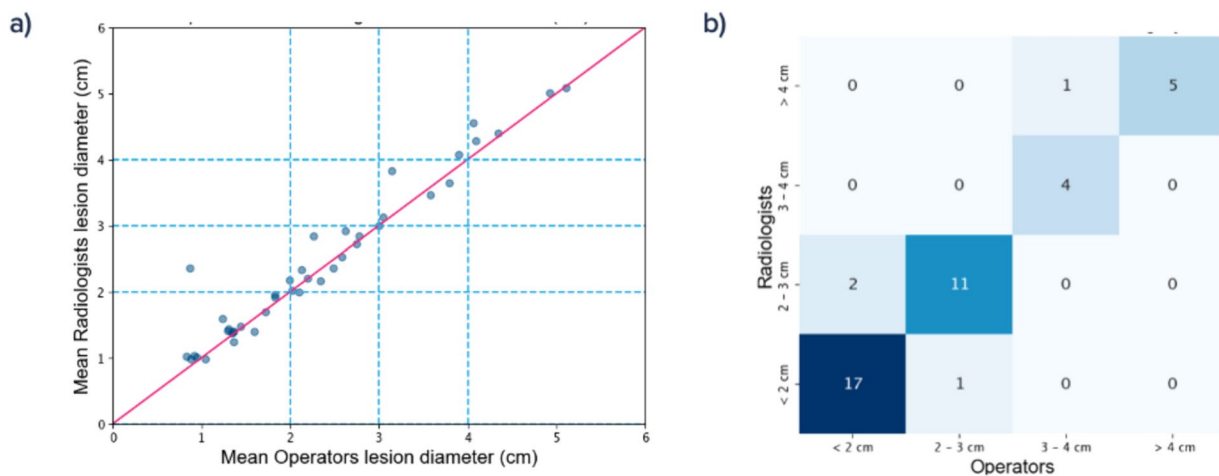


Fig. 5 Comparison of lesion size measurements between AI-assisted technicians and radiologists. **a** Scatter plot of mean lesion diameters measured by technicians and radiologists. The pink line represents perfect agreement, while the dotted light-blue lines indicate the Barcelona Clinic Liver Cancer (BCLC) staging system thresholds of 2, 3, and 4 cm. **b** Confusion matrix displaying the agreement in lesion size

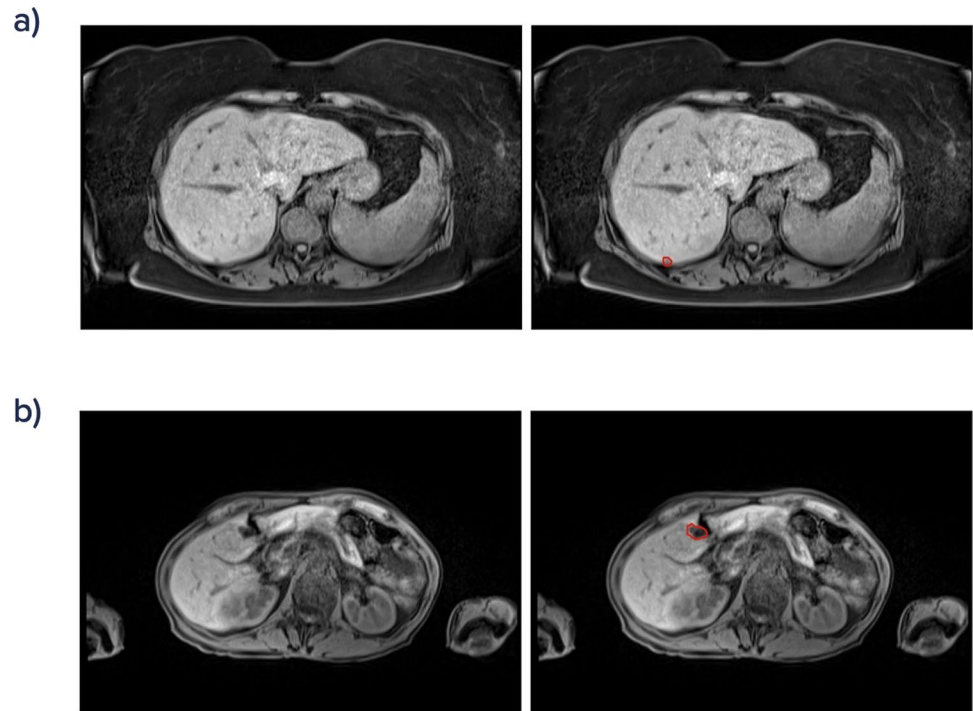
categorization based on the BCLC thresholds. The x-axis represents categories based on the mean of technicians' measurements, and the y-axis represents categories based on the mean of radiologists' measurements. The colour intensity indicates the number of lesions in each category combination, with darker shades representing higher counts

particular focus on inter-operator variability. The results showed excellent agreement between technicians and radiologists.

The participating radiologists had an average of 13 years of experience, while the technicians had backgrounds in biology but no prior experience in radiology. Despite this, the liver volumetry results demonstrate that, with appropriate training and AI assistance, technicians are capable of accurately delineating livers and partitioning the volume into Couinaud segments based on manually placed anatomical landmarks. Significantly, their results agreed strongly with those of the radiologists, with inter-rater variability similar to that observed between radiologists. With respect to lesion detection, all lesions segmented by at least two out

of three radiologists were also identified by most technicians. However, technicians detected an additional 15 structures that were not flagged by radiologists. An adjudicator panel, composed of two radiologists with 15 and 18 years of experience, assessed these structures and agreed that 7 out of these 15 identified structures were indeed lesions; the remaining 8 structures were deemed to be non-lesion, representing inconsequential, benign findings such as partial volume artifacts or blood vessels (Example in Fig. 6). Among the lesions delineated by most participants in both groups, there was remarkable consistency in terms of diameter and Couinaud location, indicating large independence of the analyst, minimizing the potential for variations that could affect treatment decisions and planning based on

Fig. 6 Example of structures segmented by technicians but not by radiologists. **a** Adjudicated by panel as lesion. **b** Adjudicated by panel as not-lesion



lesion characteristics. Discrepancies between the groups were lower than those measured within each group, primarily because accuracy samples are based on the mean of three measurements, whereas group variabilities compare single measurements. Variability within both groups was comparable for lesion diameter categorization and location in Couinaud segments. Despite similar overall accuracies in lesion detection, the technicians group exhibited a tendency towards over-detection compared to radiologists, who had a higher specificity. Their agreement was partly aided by the initial mask provided by the AI model, which has been shown to increase agreement [14]. To further refine the pipeline for clinical deployment, a final review step by a radiologist could be introduced, focusing on removing false-positive lesions flagged by technicians.

To address the challenges of radiology in recent times, new clinical strategies are being explored, such as radiologists overseeing pre-calculated outputs and employing personnel with lower levels of specialization, while integrating AI-based tools. Several studies have highlighted the potential of integrating AI with non-specialist personnel in radiology. For instance, Sullivan et al. demonstrated that technologists could effectively perform total metabolic tumor volume measurements with AI assistance [16]. Similarly, Suman et al. (2020) found that trained technologists could reliably conduct volumetric pancreas segmentation on CT images [17]. In the field of RECIST measurements, Gouel et al. showed high reproducibility when technologists performed RECIST 1.1 measurements in breast cancer follow-up [18], supported by Beaumont et al., who

optimized workflows for RECIST assessments [19]. Studies have also shown that non-specialists can accurately quantify arterial obstruction in pulmonary embolism [20] and measure leg length discrepancies [21]. AI integration has significantly improved lesion detection accuracy in various contexts, including real-time skin lesion assessment, colonoscopy for diminutive polyp identification, and breast cancer detection in mammography [22–24]. These advancements underscore the potential for AI to support less specialized personnel in complex diagnostic tasks. Building on this foundation, our study demonstrates high agreement levels between radiologists and technicians in liver volumetry and lesion detection during liver resection. This suggests that AI-assisted non-specialist personnel can effectively reduce the workload on radiologists without compromising diagnostic accuracy. By leveraging AI tools, radiology departments can potentially optimize workflow efficiency and improve diagnostic outcomes.

The integration of AI into the workflow potentially bridges a proficiency gap, ensuring high-quality analysis and diagnosis even when highly skilled radiologists are not directly involved. By leveraging the strengths of AI and the human element provided by technicians, a more efficient and accessible diagnostic process is facilitated, optimizing the utilization of available radiological expertise. Furthermore, implementing an AI-assisted technician approach in radiology departments could potentially lead to cost savings. By reducing the reliance on highly specialized radiologists for routine tasks and improving workflow efficiency, this approach could enable radiology

departments to handle a higher volume of cases without compromising quality.

This study has several limitations. First, the sample size of 18 cases is relatively small, and the range of liver pathologies analyzed was limited, focusing primarily on patients with colorectal liver metastases. A larger dataset with a wider variety of clinical scenarios, such as primary liver tumors and other metastatic origins, would strengthen the assessment of the AI-assisted technician approach and improve the generalizability of the findings. Second, the image dataset was confined to one scanner model and manufacturer, though our experience suggests this is not a severe limitation. Third, as the study aims to assist in treatment decision-making and planning for patients previously diagnosed with liver cancer, the operators were aware of the presence of at least one lesion. Providing diagnostic clinical information prior to the execution of the pipeline could further improve the specificity of the operators. Finally, a comparison between radiologists with and without AI assistance would have been valuable to evaluate the effect of the assistance and potential time reduction. Addressing these limitations in future studies would provide a more comprehensive evaluation of the AI-assisted technician approach in liver cancer imaging.

In conclusion, this study suggests that AI-assisted technicians can achieve performance comparable to radiologists in liver segmentation, Couinaud division, and lesion detection. While this approach may improve radiology department efficiency, it is important to consider the AI results alongside patient clinical information. Radiologist supervision remains essential for interpreting the AI output within the broader clinical context and making final patient management decisions. Future studies should explore the integration of AI-assisted technicians into clinical workflows, assessing both quantitative performance and impact on patient outcomes.

Open Access This article is licensed under a Creative Commons Attribution-NonCommercial-NoDerivatives 4.0 International License, which permits any non-commercial use, sharing, distribution and reproduction in any medium or format, as long as you give appropriate credit to the original author(s) and the source, provide a link to the Creative Commons licence, and indicate if you modified the licensed material. You do not have permission under this licence to share adapted material derived from this article or parts of it. The images or other third party material in this article are included in the article's Creative Commons licence, unless indicated otherwise in a credit line to the material. If material is not included in the article's Creative Commons licence and your intended use is not permitted by statutory regulation or exceeds the permitted use, you will need to obtain permission directly from the copyright holder. To view a copy of this licence, visit <http://creativecommons.org/licenses/by-nc-nd/4.0/>.

References

1. J. Ferlay *et al.*, 'Cancer incidence and mortality worldwide: Sources, methods and major patterns in GLOBOCAN 2012', *International Journal of Cancer*, vol. 136, no. 5, pp. E359–E386, 2015, <https://doi.org/10.1002/ijc.29210>.
2. 'Global cancer statistics, 2012 - Torre - 2015 - CA: A Cancer Journal for Clinicians - Wiley Online Library'. Accessed: Jan. 16, 2024. [Online]. Available: <https://acsjournals.onlinelibrary.wiley.com/doi/full/https://doi.org/10.3322/caac.21262>
3. A. Ananthakrishnan, V. Gogineni, and K. Saeian, 'Epidemiology of Primary and Secondary Liver Cancers', *Semin Intervent Radiol*, vol. 23, no. 1, pp. 47–63, Mar. 2006, <https://doi.org/10.1055/s-2006-939841>.
4. M. Reig, 'BCLC strategy for prognosis prediction and treatment recommendation: The 2022 update', *Journal of Hepatology*, vol. 76, 2022
5. J. K. Heimbach *et al.*, 'AASLD guidelines for the treatment of hepatocellular carcinoma', *Hepatology*, vol. 67, no. 1, pp. 358–380, 2018, <https://doi.org/10.1002/hep.29086>.
6. P. R. Galle *et al.*, 'EASL Clinical Practice Guidelines: Management of hepatocellular carcinoma', *Journal of Hepatology*, vol. 69, no. 1, pp. 182–236, Jul. 2018, <https://doi.org/10.1016/j.jhep.2018.03.019>.
7. M. Omata *et al.*, 'Asia-Pacific clinical practice guidelines on the management of hepatocellular carcinoma: a 2017 update', *Hepatol Int*, vol. 11, no. 4, pp. 317–370, Jul. 2017, <https://doi.org/10.1007/s12072-017-9799-9>.
8. J. Martin *et al.*, 'Colorectal liver metastases: Current management and future perspectives', *World J Clin Oncol*, vol. 11, no. 10, pp. 761–808, Oct. 2020, <https://doi.org/10.5306/wjco.v11.i10.761>.
9. 'Radiologist shortage leaves patient care at risk, warns royal college - ProQuest'. Accessed: Jan. 16, 2024. Available: <https://www.proquest.com/openview/ff4e0a3098380a9f39485f360c19bebc/1?pq-origsite=gscholar&cbl=2043523>
10. A. B. Rosenkrantz, D. R. Hughes, and R. Duszak, 'The U.S. Radiologist Workforce: An Analysis of Temporal and Geographic Variation by Using Large National Datasets', *Radiology*, vol. 279, no. 1, pp. 175–184, Apr. 2016, <https://doi.org/10.1148/radiol.2015150921>.
11. R. J. M. Bruls and R. M. Kwee, 'Workload for radiologists during on-call hours: dramatic increase in the past 15 years', *Insights Imaging*, vol. 11, no. 1, p. 121, Nov. 2020, <https://doi.org/10.1186/s13244-020-00925-z>.
12. N. Akyurt, 'Job satisfaction and perceived stress among radiology technicians: a questionnaire survey in relation to sociodemographic and occupational risk factors', *Int Arch Occup Environ Health*, vol. 94, no. 7, pp. 1617–1626, Oct. 2021, <https://doi.org/10.1007/s00420-021-01667-1>.
13. C. R. Bailey, A. M. Bailey, A. S. McKenney, and C. R. Weiss, 'Understanding and Appreciating Burnout in Radiologists', *RadioGraphics*, vol. 42, no. 5, pp. E137–E139, Sep. 2022, <https://doi.org/10.1148/rg.220037>.
14. N. Vogt *et al.*, 'A Deep-Learning Lesion Segmentation Model that Addresses Class Imbalance and Expected Low Probability Tissue Abnormalities in Pre and Postoperative Liver MRI', in *Medical Image Understanding and Analysis*, G. Yang, A. Aviles-Rivero, M. Roberts, and C.-B. Schönlieb, Eds., in Lecture Notes in Computer Science. Cham: Springer International Publishing, 2022, pp. 398–411. https://doi.org/10.1007/978-3-031-12053-4_30.
15. A. Mojtahed *et al.*, 'Repeatability and reproducibility of deep-learning-based liver volume and Couinaud segment volume

- measurement tool', *Abdom Radiol (NY)*, Oct. 2021, <https://doi.org/10.1007/s00261-021-03262-x>.
16. J. Sullivan, C. Olson, M. Thorpe, G. Johnson, M. Jain, and J. Young, 'Technologist Based Implementation of Total Metabolic Tumor Volume into Clinical Practice', *Journal of Nuclear Medicine*, vol. 62, no. supplement 1, pp. 176–176, May 2021.
 17. G. Suman *et al.*, 'Development of a volumetric pancreas segmentation CT dataset for AI applications through trained technologists: a study during the COVID 19 containment phase', *Abdom Radiol*, vol. 45, no. 12, pp. 4302–4310, Dec. 2020, <https://doi.org/10.1007/s00261-020-02741-x>.
 18. P. Gouel *et al.*, 'Evaluation of the capability and reproducibility of RECIST 1.1. measurements by technologists in breast cancer follow-up: a pilot study', *Sci Rep*, vol. 13, no. 1, Art. no. 1, Jun. 2023, <https://doi.org/10.1038/s41598-023-36315-w>.
 19. H. Beaumont *et al.*, 'Radiology workflow for RECIST assessment in clinical trials: Can we reconcile time-efficiency and quality?', *European Journal of Radiology*, vol. 118, pp. 257–263, Sep. 2019, <https://doi.org/10.1016/j.ejrad.2019.07.030>.
 20. 'Frontiers | Can a Trained Radiology Technician Do Arterial Obstruction Quantification in Patients With Acute Pulmonary Embolism?' Accessed: Jan. 16, 2024. Available: <https://www.frontiersin.org/articles/https://doi.org/10.3389/fcvm.2019.00038/full>
 21. S. A. White, S. Shellikeri, M. L. Muñoz, J. C. Edgar, J. C. Nguyen, and R. W. Sze, 'Can Radiology Technologists be Trained to Measure Leg Length Discrepancies as Accurately as Pediatric Radiologists?', *Academic Radiology*, vol. 29, no. 1, pp. 51–55, Jan. 2022, <https://doi.org/10.1016/j.acra.2020.09.020>.
 22. 'Real-world post-deployment performance of a novel machine learning-based digital health technology for skin lesion assessment and suggestions for post-market surveillance'. Accessed: Jan. 16, 2024. Available: <https://www.researchsquare.com>
 23. 'Real-Time Use of Artificial Intelligence in Identification of Diminutive Polyps During Colonoscopy: A Prospective Study - PubMed'. Accessed: Jan. 16, 2024. Available: <https://pubmed.ncbi.nlm.nih.gov/30105375/>
 24. M. Sasaki *et al.*, 'Artificial intelligence for breast cancer detection in mammography: experience of use of the ScreenPoint Medical Transpara system in 310 Japanese women', *Breast Cancer*, vol. 27, no. 4, pp. 642–651, Jul. 2020, <https://doi.org/10.1007/s12282-020-01061-8>.

Publisher's Note Springer Nature remains neutral with regard to jurisdictional claims in published maps and institutional affiliations.